Computation of moments in quadratic discontinuous anisotropic plane elasticity fast multipole formulation

J. S. França[1,4], L. S. Campos[2], A. B. Dias Jr.[3], D. D. C. Matheus, E. L. Albuquerque[4]

[1]*Federal University of West Bahia*
Rua Professor José Seabra de Lemos, Recanto dos Pássaros, 47808-021, Bahia, Brazil.
jailson.santos@ufob.edu.br
[2]*Federal University of Espírito Santo*
Av. Fernando Ferrari, Goiabeiras, 29075-910, Espírito Santo, Brazil.
lucas.s.campos@ufes.br
[3]*Institute Federal of Brasilia, Campus Estrutural*
Scia, Guará, Brasília - DF, 73340, Brazil
afonso.dias@etfbsb.edu.br.
[4]*Faculty of Technology, University of Brasilia*
Asa Norte, 70910-900, Brasilia, Brazil
danilodchaves.m@gmail.com, eder@unb.br.

Abstract. The fast multipole formulation is used in order to solve large scale problems in general boundary element formulation. In this work we will present the computation of moments in the anisotropic plane elasticity fast multipole formulation with quadratic discontinuous elements. Fundamental solutions of plane elasticity are represented by complex functions from the classical 2D elasticity theory. The Multipole Expansion for kernels **U** (displacement field) and **T** (traction field) will be computed using series. The convergence of the series expansion to the fundamental solutions is analyzed considering different numbers of series terms and different distance from source point to field point. Moments are computed to evaluate integrals of influence matrices where elements are far away from the source point, whereas the conventional approach will be applied to evaluate the integrals on the remaining elements that are closer to the source point. All fast multipole operations are demonstrated in this work and compared to the standard boundary element formulation.

Keywords: anisotropic plane elasticity, fast multipole method, boundary element method, quadratic discontinuous elements.

1 Introduction

Numerical techniques are auxiliary techniques that aim to present results so good as analytical results. However, numerical techniques in their great majority have advantages and disadvantages. The Boundary Elements Method - BEM, [1], is an excellent numerical method because it is very easy to model problems with complex geometries, and also for semi-infinite and infinite domains. It also stands out for being able to reduce the simulation domain, as it is only necessary to discretize the model's contours. However, BEM produces full and non-symmetric matrices, generating a high computational cost for assembling and solving the linear system. This restricts the use of BEM for applications in problems with few degrees of freedom (DOFs), which makes it a less competitive method, for example, when compared to the Finite Element Method.

Several acceleration techniques applied to BEM have been investigated and applied in the most diverse areas of engineering for large-scale problems, in order to place BEM with a competitive method. The technique discussed in this work is the Fast Multipole Method - FMM, [2]. This technique was developed by Rokhlin and Greengard [3–5], and aims to speed up BEM solutions several times, reducing CPU time and memory used for construction and solving the linear system to $O(N \log N)$. The BEM associated with the FMM, here called the FMBEM, is a great tool to solve large-scale problems.

According to [2], the FMBEM idea is to transform node-to-node interactions into cell-to-cell interactions, and in the end, these cells have a hierarchical structure. In addition, the kernel of the fundamental solution is expanded into series. As consequence, two groups of integrals are generated, the called near (adjacent) which are solved by the conventional BEM, which we will discretize into discontinuous quadratic elements, and the well separated and distant integrals which will be solved by the FMBEM. Therefore, the objective of this work is to present the steps for the FMBEM based on the expansion of fundamental solutions to an anisotropic problem and to show that the FMM can be a good technique to associate with the BEM.

2 Boundary Elements for anisotropic materials

Consider an integral equation that relates a fundamental state to any other state in a body with domain Ω and contour Γ, written for an interior point of domain [6]:

$$u_i + \int_\Gamma T_{ij} u_j d\Gamma = \int_\Gamma U_{ij} t_j d\Gamma + \int_\Omega P_j U_{ij} d\Omega \tag{1}$$

where, u_j and t_j are the displacement and traction vectors, respectively. The material of the domain is anisotropic. The source point z_0 **(x)** is a point to which a unit point force P is applied. The responses of this body at any field point z **(y)** due to this unit force are the displacement and traction fundamental solutions given by U_{ij} and T_{ij}, respectively. Figure 2 taken from [2], shows the relation of the change of coordinate (x, y) to complex notation (z_0, z).

2.1 Fundamental solutions

For 2D plane-stress problems, the fundamental solution of the displacement U_{ij} and the fundamental solution of traction T_{ij}, which represent the displacement and the surface force at the point field z, in direction j, when the concentrated force is acting in direction i at source point z_0, are given through a mapping on a complex plane, such that:

$$U_{ij}(z, z_o) = 2Re[q_{i1} A_{j1} ln(z_{o1} - z_1) + q_{i2} A_{j2} ln(z_{o2} - z_2)], \tag{2}$$

$$T_{ij}(z, z_o) = 2Re\Big[\frac{1}{(z_{o1} - z_1)} g_{j1}(\mu_1 n_1 - n_2) A_{i1} + \frac{1}{(z_{o2} - z_2)} g_{j2}(\mu_2 n_1 - n_1) A_{i2}\Big], \tag{3}$$

where $Re[\ ]$ indicates the real part of the expression, and the terms μ_k, q_{ik}, g_{ji} and A_{jk} can be consulted in [7].

2.2 Boundary integral equation

It is possible to transform in Eq. (1) the domain integral a boundary integral by the radial integration method. However, let's consider here that the problem has no body force. Thus, Eq. (1) is now written in the form of Eq. (4)

$$c_{kj}(\mathbf{z_0}) u_k(\mathbf{z_0}) + \fint_\Gamma T_{kj}(\mathbf{z_0}, \mathbf{z}) u_j(\mathbf{z}) d\Gamma(\mathbf{z}) = \int_\Gamma U_{kj}(\mathbf{z_0}, \mathbf{z}) t_j(\mathbf{z}) d\Gamma(\mathbf{z}), \tag{4}$$

where c_{kj} is known as a free coefficient and $\fint$ represents an integral in the sense of the principal value of Cauchy. The fundamental solutions U_{ij} and T_{ij}, used in Eq. (4), shown in Eqs. (2) and (3), are singular when the source point z_0 tends to the field point z. In the case, Eq. (2) is weak singular and can be integrated as an improper integral, while Eq. (3) is strong singular and can be integrated on the sense of Cauchy principal value.

2.3 Discretization on discontinuous quadratic elements

For numerical solution of Eq. (4), the domain discretization in boundary elements is performed. For this, first, the displacements and tractions for each element are given by $u_k(\xi) = N_i \tilde{u}_k$ and $t_k(\xi) = N_i \tilde{t}_k$, where $\tilde{u}_k$ and $\tilde{t}_k$ are the nodal displacements and tractions at the node of the discretized mesh, and N_i are shape functions for the discontinuous quadratic elements, shown in the Eqs. (6) - (8). Thus, considering N the total number of boundary elements and replacing the terms $u_k(\xi)$ and $t_k(\xi)$ in Eq. (4), it is possible to transform the integral equation in

$$c_{kj}(\xi)u_k(\xi) + \sum_{m=1}^{N}\left[\oint_{\Gamma_i} T_{kj}(\xi, z(\xi))u_j J(\xi)d\xi\right] = \sum_{m=1}^{N}\left[\int_{\Gamma_i} U_{kj}(\xi, z(\xi))t_j J(\xi)d\xi\right]. \quad (5)$$

In Eq. (5), ξ represents a dimensionless coordinate along the quadratic element, as it is possible to see in Figure 1, the relation between the coordinate ξ and x is the graphical behavior of the N_i shape functions shown in Figure 1. The J represents the Jacobian module, as shown by [8].

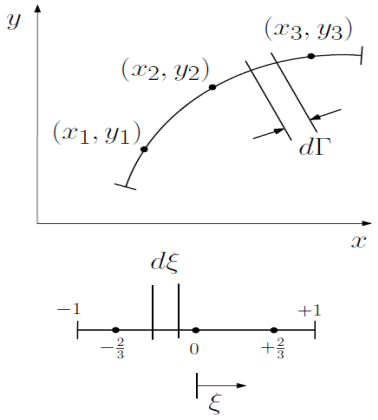

Figure 1. Transformation of coordinates $x_1 - x_2$ to ξ in discontinuous quadratic element.

$$N_1 = \left(\frac{9}{8}\xi - \frac{3}{4}\right)\xi, \qquad \frac{dN_1}{d\xi} = \frac{3}{4}\left(-1 + 3\xi\right). \quad (6)$$

$$N_2 = 1 - \frac{9}{4}\xi^2, \qquad \frac{dN_2}{d\xi} = \frac{-9}{2}\xi. \quad (7)$$

$$N_3 = \left(\frac{9}{8}\xi + \frac{3}{4}\right)\xi, \qquad \frac{dN_3}{d\xi} = \frac{3}{4}\left(1 + 3\xi\right). \quad (8)$$

Eq. (5) must be applied to each node of the discretized boundary, which, finally, will generate an algebraic system of full and non-symmetrical matrix, of type $\mathbf{Hu} = \mathbf{Gt}$, which, by reallocating the known and unknown terms, one arrives at a linear equation system of the type $Ax = b$, where $\mathbf{x}$ is the solution vector of the surface forces and displacements. When dealing with problems where there are thousands of degrees of freedom, the solution of the system $\mathbf{Ax} = \mathbf{b}$ becomes a computational challenge, both for data storage and for the solution of the problem. It is at this point that the conventional BEM becomes ineffective, so this work presents the use of a technique used to modify the way the source and field points interact with each other, called the Fast Multipole Method.

3 FMBEM for anisotropic 2D problems

As already said, Eqs. (2) and (3) have singularities. According to [2], one of the reasons for the reduction of operations in FMBEM is due to the fact that fundamental solutions of the BIEs can be expanded in the form of series in a complex plane as shown in Figure 2.

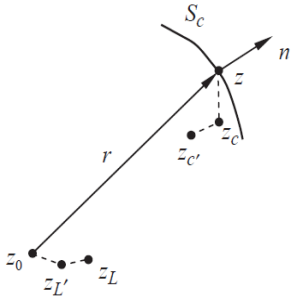

Figure 2. Complex notation and the related points for fast multipole.

$$G(z_0, z) = \sum_{k=0}^{\infty} O_k(z_0 - z_c)I_k(z - z_c), \quad \begin{cases} I_k(z) = \frac{z^k}{k!}, & k \geq 0 \\ O_k(z)\begin{cases} -log(z), & k = 0 \\ \frac{(k-1)!}{z^k}, & k \geq 1 \end{cases} \end{cases} \quad (9)$$

$$G'(z_0, z) = \sum_{k=1}^{\infty} O_k(z_0 - z_c)I_{k-1}(z - z_c), \quad I_{k-1}(z)\begin{cases} I'_k(z) = 0, & k = 1 \\ I'_k(z) = \frac{k(z^{k-1})}{k!}, & k > 1 \end{cases} \quad (10)$$

For the expansion of the anisotropic fundamental solution $\mathbf{U}$ and $\mathbf{T}$, the Green operator $G(z_0, z) = log(z_0 - z)$ and its derivative $G'(z_0, z) = \frac{1}{(z_0 - z)}$ are used. To expand the fundamental solutions, an expansion point z_c is introduced close to the field point z, as shown in Figure 2. Calling $G(z_0, z) = log(z - z_c - z_0 + z_c)$, applying the

Taylor series expansion, and performing the algebraic steps of [9], the final expression of the Green term is given by (9), and its derivative in the form of Eq. (10).

3.1 FMBEM operations for U and T fundamental soluitons

Multipolar expansion: Let's introduce an intermediate point z_{ci} for the coordinate (z_{c1}, z_{c2}) near the point field (z_1, z_2), as you can be seen in Figure 2. So it is said that $|z_1 - z_{c1}| << |z_{o1} - z_{c1}|$ and $|z_2 - z_{c2}| << |z_{o2} - z_{c2}|$. Thus, using the expansion of Eqs. (9) and (10) and substituting in the fundamental solution of **U** and **T**, Eqs. (2) and (3) and integrating them according to the terms of Eq. (4), we arrive in the multipolar expansion for both cases, written as Eqs. (11) and (12), for $m = 1, 2$ and $k \geq 0$.

$$2Re \sum_{k=0}^{\infty} O_k(z_{om} - z_{cm}) \underbrace{\int_{S_c} t_j q_{im} A_{jm} I_k(z_m - z_{cm}) dS.}_{\text{kernel U}\rightarrow M_k(z_{cm}):\, moment} \tag{11}$$

$$2Re \sum_{k=0}^{\infty} O_k(z_{om} - z_{cm}) \underbrace{\int_{S_c} u_j g_{im}(\mu_m n_1 - n_2) A_{jm} I_{k-l}(z_m - z_{cm}) dS.}_{\text{kernel T}\rightarrow \tilde{M}_k(z_{cm}):\, moment} \tag{12}$$

After discretizing the contour S, the hierarchical tree is constructed. This step is about building rectangles/cell until the amount of 1 node for each cell is reached, and thus the hierarchical tree is built with the parent and child cells.

Moment to Moment (M2M): now, assuming that the points z'_{c1} and z'_{c2} are the points where z_{c1} and z_{c2} have been moved. With that, two new moments can be calculated. Therefore the M2M translation for the integral of the fundamental solution **U** and **T** are written as:

$$M_k(z'_{cm}) = \sum_{l=0}^{k} I_{k-l}(z_{cm} - z'_{cm}) \underbrace{\int_{S_c} t_j q_{im} A_{jm} I_l(z_m - z_{cm}) dS,}_{\text{kernel U}\rightarrow M_{l_2}(z_{cm})} \tag{13}$$

$$\tilde{M}_k(z'_{cm}) = \sum_{l=0}^{k} I_{k-l}(z_{cm} - z'_{cm}) \underbrace{\int_{S_c} u_j g_{im}(\mu_m n_1 - n_2) A_{jm} I_l(z_m - z_{cm}) dS,}_{\text{kernel T}\rightarrow \tilde{M}_{l_2}(z_{cm})} \tag{14}$$

for $m = 1, 2$ and $k \geq 0$. This step ois called upward, which involves grouping the field points "considered distant" from the source point.

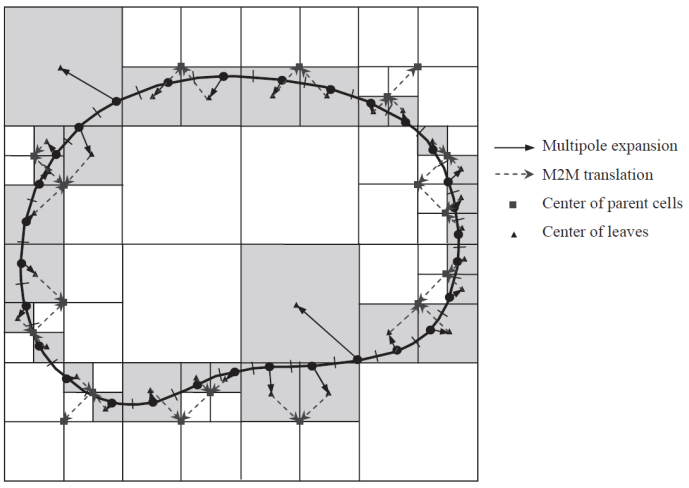

Figure 3. Upward pass: Multipole expansions and M2M translations

As shown in Figure 3, first the node of a leaf cell is transferred to its respective central point. This is carried out by inserting an intermediate point near the field point, and with that, performing the multipolar expansion, Eqs. (11) and (12), as shown in Figure 3 taken from [2]. Then, to the cells that are not leaves, the multipole moments are calculated by adding the moments multipoles of each daughter cell, applied to the parent cell, thus performing the M2M translation, through Eqs. (13) and (14).

Moment to local (M2L): after the two steps of expansions on the field point, we will now expand on the source point. Considering two points z_{L1} and z_{L2} near the source point (z_{o1}, z_{o2}), as can be seen in an analogy in Figure 2. Thus, considering that $|z_{oi} - z_{Li}| << |z_{Li} - z_{ci}|$, the equation for the M2L translation is written as:

$$2Re\int_{S_c} t_j\left[q_{im}A_{jm}G(z_{om},z_m)\right]dS = 2Re\left[\underbrace{\sum_{l=0}^{\infty}(-1)^k\left[\sum_{k=0}^{\infty}O_{km+lm}(z_{Lm}-z_{cm})I_{lm}(z_{om}-z_{cm})\right]M_{km}(z_{cm})}_{\text{kernel U}\rightarrow L_{km}(z_{Lm}):M2L}\,I_{lm}(z_{om}-z_{cm})\right], \quad (15)$$

$$2Re\int_{S_c} u_j\left[g_{im}(\mu_m n_1 - n_2)A_{jm}G'(z_{om},z_m)\right]dS = 2Re\left[\underbrace{\sum_{l=0}^{\infty}(-1)^k\left[\sum_{k=0}^{\infty}O_{km+lm}(z_{Lm}-z_{cm})I_{lm}(z_{om}-z_{cm})\right]\tilde{M}_{km}(z_{cm})}_{\text{kernel T}\rightarrow \tilde{L}_{km}(z_{Lm}):M2L}\,I_{lm}(z_{om}-z_{cm})\right]. \quad (16)$$

Eq. (15) and (16) are called local expansion, and is valid for $m = 1, 2$ and $k \geq 0$. This step is the union of the upward process with the downward step, the downward being the second part of the hierarchical structure of the trees. With the fields points grouped in step M2M, we will now use it to iterate with the source point, through step M2L, through Eqs. (15) and (16). Figure 4 on the left shows an illustration of this process.

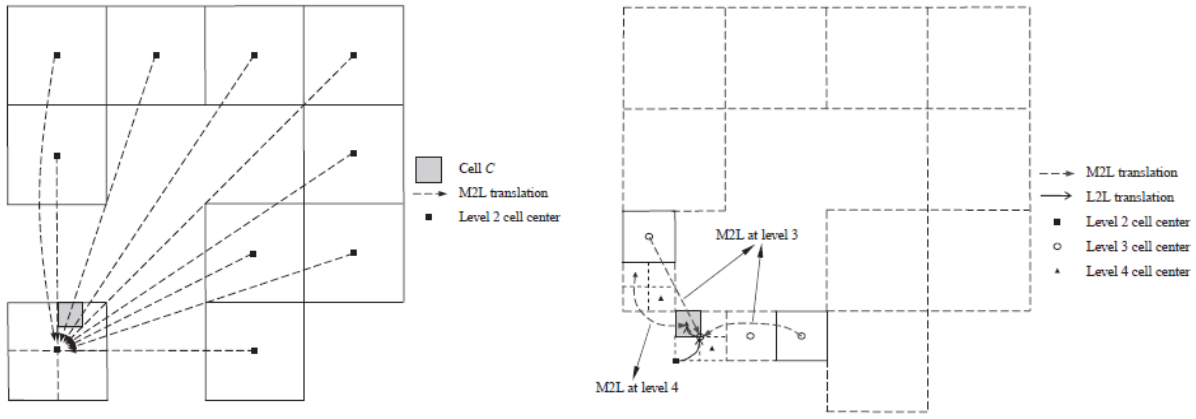

Figure 4. Left: Downward pass: M2L for level 2. Right: Downward pass: L2L for level 3 and 4.

Local to local (L2L): finally, considering the translation of the points z_{L1} and z_{L2} to the respective points z'_{L1} and $'z2_{L2}$, as shown in the illustration in Figure 2, we can write the equations for this step as

$$2Re\int_{S_c} t_j\left[q_{im}A_{jm}G(z_{om},z_m)\right]dS = 2Re\left[\underbrace{\sum_{l=0}^{p}\sum_{k=0}^{p-l}I_m(z'_{Lm}-z_L)L_{l+k}(z_{lm})}_{\text{kernel U}\rightarrow L_{km}(z'_{Lm}):L2L}\,I_{pm}(z_{mo}-z'_{Lm})\right] \quad (17)$$

$$2Re\int_{S_c} u_j\left[g_{im}(\mu_m n_1 - n_2 A_{jm}G(z_{om},z_m)\right]dS = 2Re\left[\underbrace{\sum_{l=0}^{p}\sum_{k=0}^{p-l}I_m(z'_{Lm}-z_L)L_{l+k}(z_{lm})}_{\text{kernel T}\rightarrow \tilde{L}_{km}(z'_{Lm}):L2L}\,I_{pm}(z_{mo}-z'_{Lm})\right] \quad (18)$$

Eqs. (17) and (18) demonstrate the last step for the FMBEM process, in which the L2L translation is performed for cells considered distant from level 3, as shown in the illustration in Figure 4 on the right.

The algorithm for FMBEM is then written based on adjacent cells (if they have at least one common vertex), well separated (if they are not adjacent at the same step), and far (if the parent cells are not adjacent at the same step). Adjacent phase cells are calculated directly using the BEM and those well separated and far are calculated using the steps of the FMBEM. Further details of the equations presented in section 3 can be found in [7], all theory can be found in [2], an algorithm for the steps of FMBEM can be found in [10] and in [11].

4 Results and discussions

As first results, Figure 5 shows the behavior of the exact Green operator $G(z_0, z) = \log(z_0 - z)$, with the Green operator expanded in different numbers of terms in the series. We can say that, if these results are satisfactory, then Green's term inserted in the fundamental solutions **U** and **T** will also be.

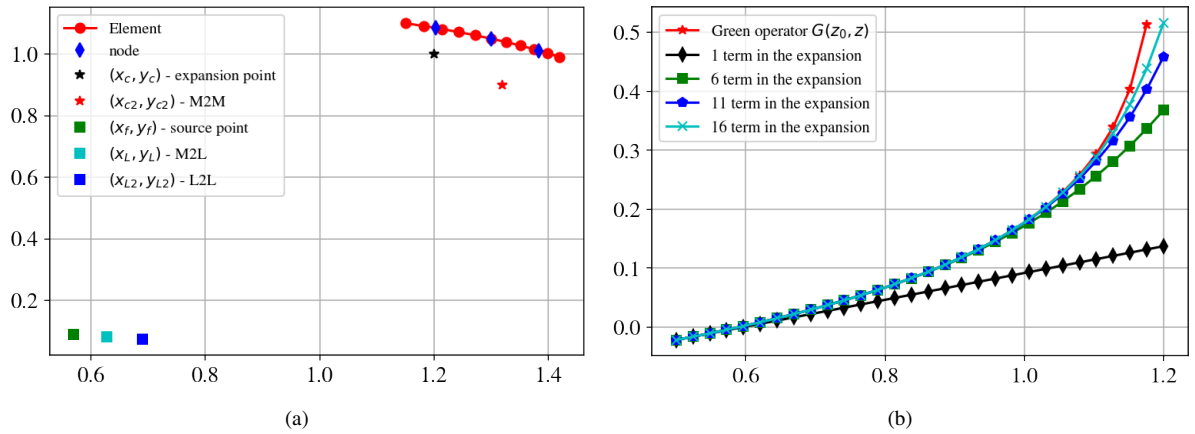

Figure 5. (a) Expansion points and FFMBEM steps. (b) Analytical expansion of Green's operator and FMBEM expansions for different terms.

The curves in Figure 5b show the convergence while an increasing number of terms are inserted in the expansion, thus presenting satisfactory results for this first analysis. These results also demonstrate importance for the subsequent phases of the FMBEM, since they start from the first stage, moment, through the expansions of the fundamental solutions.

Now we are going to validate the all implemented algorithm, both the conventional BEM that solves through discontinuous quadratic elements, and all the steps of the FMM: moment, M2M, M2L, and L2L. For this verification, we will analyze the results of some elements of the **G** and **H** matrices produced by FMBEM and compared to BEM. Considering the source point (x_f, y_f) and the field point (x_c, y_c), as can be seen in Figure 5a. Then, we calculate the moment, the first step of the method, with respect to the expansion point (x_c, y_c), then use the step M2M to perform the translation to the coordinate (x_{c2}, y_{c2}). In the next step, M2L is used to calculate the local expansion L at the coordinate (x_L, y_L), then, L2L is used to translate the expansion to (x_{L2}, y_{L2}). Finally, the local expansion is used to compute matrices **G** and **H** at the source point (x_f, y_f).

The table 1 presents the anisotropic properties for numerical computational simulation of the results. In Table 2 is shown the results for the values of matrices **G** and **H**, calculated by BEM and by the FMBEM process. The percentage error shows an excellent agreement for the FMBEM over the numbers of the terms of the series, when compared to that calculated by the BEM.

Layers	E_1 (GPa)	E_2 (GPa)	G_{12} (GPa)	ν_{12}	θ
1	2.2	4.4	0.7692	0.4286	15
2	2.2	4.4	0.7692	0.4286	-25

Table 1. Composite material properties.

Number of terms	G_1	Error	G_2	Error
2	- 0.00159443	1.14244000e-03	0.0047016	2.72520000e-04
3	- 0.00143211	8.06600235e-06	0.00457484	4.44934941e-06
4	- 0.00143095	1.61879271e-08	0.00457687	1.08086567e-08
8	- 0.00143096	5.81749508e-08	0.00457688	4.71247937e-09
BEM	**-0.00143095**		**0.00457687**	
Number of terms	H_1	**Error**	H_2	**Error**
2	- 0.01692327	1.77540000e-04	- 0.01892752	3.70520000e-04
3	- 0.01722150	4.44782431e-06	- 0.01824397	4.00248902e-06
4	- 0.01722972	3.22416705e-07	- 0.01825156	1.58399560e-07
8	- 0.01722970	3.12768830e-07	- 0.01825161	1.80890586e-07
BEM	**-0.01722916**		**-0.01825128**	

Table 2. Comparison between FMBEM and BEM.

5 Conclusions

This work has shown the steps for accelerating the BEM discretized in discontinuous quadratic elements by the FMM, in an anisotropic material problem. Green's term expansions proved to be satisfactory, which gives good confidence for good approximations of the fundamental solutions **T** and **U**. Finally, the elements of the **G** and **H** matrices that were calculated by the FMBEM proved to have good convergence, while the quantity of terms in the series of was increased. This fact will contribute to a future work in which the terms of the matrix **G** and **H** will be calculated in FMBEM analyses of anisotropic material large-scale problems.

References

[1] J. T. Katsikadelis. *The boundary element method for engineers and scientists: theory and applications*. Academic Press, 2016.
[2] Y. Liu. *Fast multipole boundary element method: theory and applications in engineering*. Cambridge university press, 2009.
[3] V. Rokhlin. Rapid solution of integral equations of classical potential theory. *Journal of computational physics*, vol. 60, n. 2, pp. 187–207, 1985.
[4] L. Greengard and V. Rokhlin. A fast algorithm for particle simulations. *Journal of computational physics*, vol. 73, n. 2, pp. 325–348, 1987.
[5] L. Greengard. *The rapid evaluation of potential fields in particle systems*. MIT press, 1988.
[6] P. Fedelinski, M. Aliabadi, and D. Rooke. The dual boundary element method in dynamic fracture mechanics. *Engineering Analysis with Boundary Elements*, vol. 12, n. 3, pp. 203–210, 1993.
[7] A. D. Junior, E. L. Albuquerque, and dos A. Reis. Computation of moments in the anisotropic plane elasticity fast multipole formulation. *Linhas Críticas*, vol. 2, n. 6, pp. 152–169, 2016.
[8] C. A. Brebbia and J. Dominguez. *Boundary elements: an introductory course*. WIT press, 1994.
[9] A. C. M. Reis and E. L. Albuquerque. *Series expansions of anisotropic plane elasticity fundamental solution*. In International Conference on Boundary Element and Meshless Techniques., 2013.
[10] S. Pfalzner and P. Gibbon. *Many-body tree methods in physics*. Cambridge University Press, 2005.
[11] V. Anisimov and J. J. Stewart. *Introduction to the Fast Multipole Method: Topics in Computational Biophysics, Theory, and Implementation*. CRC Press, 2019.